Terahertz time-domain spectroscopy of water vapor

Martin van Exter, Ch. Fattinger, and D. Grischkowsky

IBM Watson Research Center, P.O. Box 218, Yorktown Heights, New York 10598

Received April 24, 1989; accepted August 3, 1989

We describe the application of a new high-brightness, terahertz-beam system to time-domain spectroscopy. By analyzing the propagation of terahertz electromagnetic pulses through water vapor, we have made what we believe are the most accurate measurements to date of the absorption cross sections of the water molecule for the nine strongest lines in the frequency range from 0.2 to 1.45 THz.

Recently several new sources of freely propagating electromagnetic pulses have been demonstrated[1–3]; the spectral content of these sources extends from low frequencies to the terahertz frequency range. Using an optical approach in which a transient Hertzian dipole was tightly coupled to a sapphire collimating lens, we produced beams of single-cycle 0.5-THz pulses.[3] With the addition of paraboloidal focusing and collimating mirrors,[4] the resulting system has high brightness and extremely high collection efficiency.

In this Letter we describe the application of this new high-brightness system to time-domain spectroscopy[5–8] by studying the propagation of terahertz beams through water vapor. Fourier analysis of the directly measured electric fields of the propagated pulses, with and without water vapor in the beam path, yields the absorption and dispersion of water vapor as a function of frequency. This technique has some powerful advantages in producing results that appear to be equivalent to those of traditional cw spectroscopy. First, the detection of the far-infrared radiation is extremely sensitive. Although the energy per terahertz pulse is very low (1 aJ), the 100-MHz repetition rate and the coherent detection allow us to determine the electric field of the propagated pulse with a signal-to-noise ratio of ~3000 for an integration time of 125 msec. In terms of average power this sensitivity exceeds that of liquid-helium-cooled bolometers[9] by more than 1000 times. Second, because of the gated and coherent detection, the thermal background that plagues traditional measurements in this frequency range[9] is observationally absent. These two advantages have enabled us to make what we believe are the most accurate measurements to date of the absorption cross sections of the nine strongest rotational transitions of water vapor in the frequency range from 0.2 THz (6.6 cm^{-1}) to 1.45 THz (48.4 cm^{-1}).

The terahertz radiation source[4] is illustrated in Fig. 1(a). The emitting dipolar antenna was located in the middle of a 20-mm-long transmission line consisting of two parallel 10-μm-wide aluminum lines separated from each other by 30 μm. The pattern was fabricated on an ion-implanted, silicon-on-sapphire wafer. The antenna was driven by photoconductively shorting the 5-μm antenna gap with 70-fsec pulses coming at a 100-MHz rate in a 1.5-mW beam from a colliding-pulse, mode-locked dye laser. The terahertz radiation detector[4] uses the same ultrafast antenna and terminating transmission line as the transmitter. During operation the antenna is driven by the incoming terahertz radiation pulse polarized parallel to the antenna. The induced time-dependent voltage across the antenna gap is measured by shorting the gap with the 70-fsec optical pulses in the detection beam and monitoring the collected charge (current) versus the time delay between the excitation and detection laser pulses.

The terahertz optics[4] illustrated in Fig. 1(b) consists of two matched crystalline magnesium oxide (MgO) spherical lenses in contact with the sapphire side of the silicon-on-sapphire chips located near the foci of two identical paraboloidal mirrors. The combination of the MgO lens and the paraboloidal mirror collimated the emitted radiation to beam diameters (10–70 mm) proportional to the wavelength and with a frequency-independent divergence of only 25 mrad. The second identical combination on the receiving end focused the terahertz beam onto the detector. The total path length from transmitter to receiver was 88 cm, of which 86 cm was located in an airtight enclosure in which the water-vapor content could be controlled.

Figure 2(a) displays the detected terahertz radiation pulses after propagating through 1 atm of pure nitrogen. This high signal-to-noise measurement with millivolts of signal was made in a single 10-min scan of the 200-psec relative time delay between the

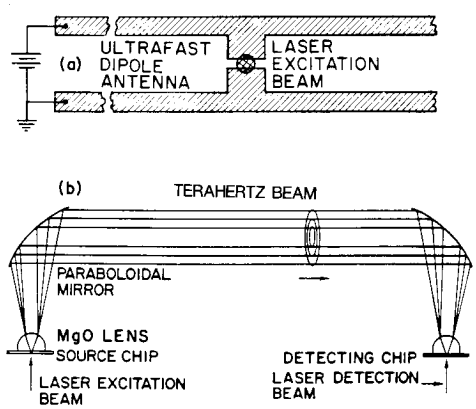

Fig. 1. (a) Ultrafast dipolar antenna. (b) Terahertz optics.

0146-9592/89/201128-03$2.00

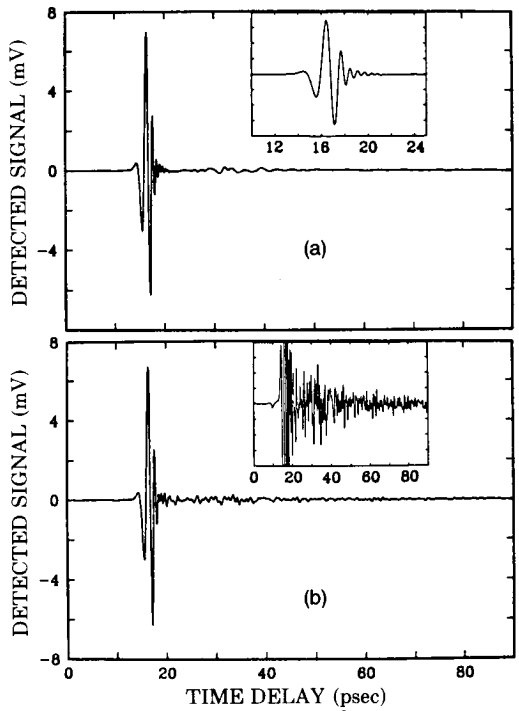

Fig. 2. (a) Measured electrical pulse of the freely propagating terahertz beam in pure nitrogen. The inset shows pulse on an expanded time scale. (b) Measured electrical pulse with 1.5 Torr of water vapor in the enclosure. The inset shows pulse on a 20× expanded vertical scale.

excitation and detection pulses. When 1.5 Torr of water vapor, corresponding to 8% humidity at 20.5°C, was added to the enclosure, the transmitted pulse changed to that shown in Fig. 2(b). The additional fast oscillations are caused by the combined action of the dispersion and absorption of the water-vapor lines. The slower and more erratic variations seen in both Figs. 2(a) and 2(b) result from reflections of the main pulse. They are reproducible and do not affect our data analysis, as they divide out in the frequency domain. The insets show the data on a 20× expanded vertical scale. Here, the oscillations are seen to decay approximately exponentially in time. For a low concentration of water vapor the observed decay corresponds to an average coherent relaxation time T_2.

The amplitude spectra of the full 200-psec scans corresponding to Figs. 2(a) and 2(b) are compared in Fig. 3(a), where the strong water-absorption lines are clearly observable. The additional structure on the spectra is not related to noise but results from reflections of the main pulse. At each line we have indicated two frequencies, our measured value and in parenthesis the accepted literature value.[10–16] Our measured line centers have an estimated error of ±0.001 THz. Within this bracket they agree with the literature values. We assign the systematic deviation of +0.1% to error in the calibration of our delay line. Our peak positions are obtained from a fit to the Fourier transform, assuming a Lorentzian line shape. The basic data are of sufficient accuracy to permit the determination of the peak position of one fifth of the 0.005-THz fundamental frequency given by the 200-psec scan duration. A numerical method of making the fit is to extend the scan artifically by the addition of zeros.[17] Using this approach, we extended the scan range to 600 psec and obtained the same line centers.

From the above spectra the corresponding absorption coefficients are displayed in Fig. 3(b). The vertical scale is the natural logarithm of the ratio of the two amplitude spectra shown in Fig. 3(a) and thus represents the amplitude absorption coefficient. In Table 1 we have converted the measured absorption into the commonly used peak-intensity absorption coefficient α_0 for a 1-m path (m^{-1}) at 100% humidity (18 Torr at 20.5°C) in 1 atm of nitrogen. These values were compiled from eight 10-min scans taken at humidities between 3% and 13%. The humidity was varied to accommodate the different line strengths.

Three lines demanded special attention. As the 1.097- and the 1.113-THz lines are relatively close together, we corrected for the overlap to get their line strengths. The measured line shape of the 1.163-THz line is asymmetric owing to the presence of two weaker modes at 1.153 and 1.158 THz. Using the theoretical strengths of these modes, we also corrected the measured absorption of this line. With our high signal-to-noise ratio the relative strengths of the lines could be determined to better than 10% with the actual uncertainty indicated in Table 1. We used a commercial

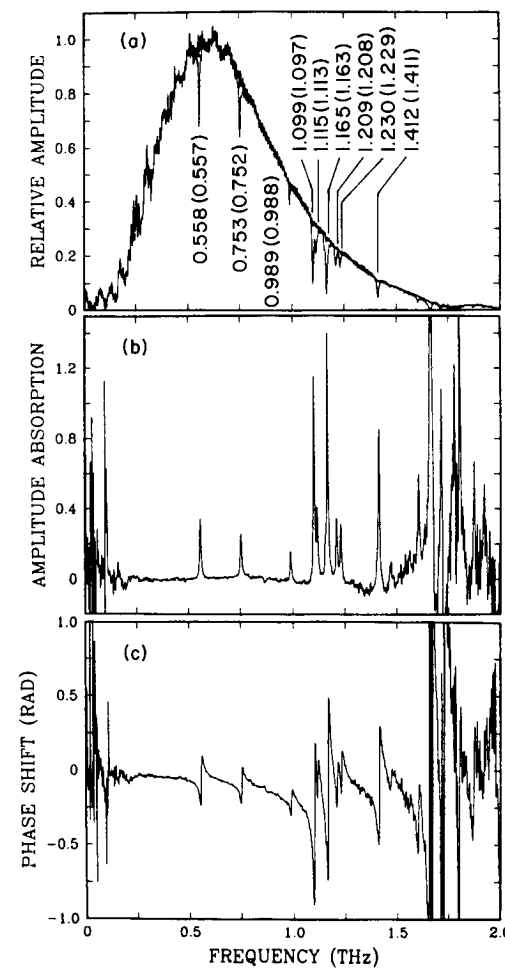

Fig. 3. (a) Amplitude spectra of Figs. 2(b) and 2(c). (b) Amplitude absorption coefficient obtained from Fig. 3(a). (c) Relative phase of the spectral components of Fig. 3(a).

Table 1. Comparison of Our Experimental Results with Theoretical Predictions for the Indicated Lines (in terahertz)[a]

Line	Exp α_0	10	11	12	13*	14*	15*	16*
0.557	9.4 (2)	9.6	9.9	8.6	4.6	10.8		9.7
0.752	6.9 (4)	6.8	6.9	5.9	5.1	7.1		6.8
0.988	5.0 (4)	5.0	5.1	4.3	2.2	5.3	5.1	5.0
1.097	32.0 (10)	33.8	34.3		33.8	33.8	33.8	33.8
1.113	10.1 (7)	10.2	10.5		1.5	10.3	10.1	10.3
1.163	37.9 (14)	38.2	39.1		36.7	38.6	35.9	38.2
1.208	9.8 (7)	12.9			14.7	12.1	11.2	12.8
1.229	8.5 (7)	10.0			7.1	10.5	9.7	10.0
1.410	23.1 (30)	30.5			45.9	31.6	29.4	30.2

[a] Asterisks indicate relative values only.

hygrometer (Fischer Scientific 11-661-7A) to determine the relative humidity inside the enclosure, and, using that value, we evaluated the absolute absorption strength to within 10%. In the last seven columns of Table 1 we present theoretical values for the peak absorption coefficient α_0 extracted from the literature. The values of Ref. 10 appear to be the most reliable, as they result from a substantial compilation of data. Because Ref. 10 cites the absorption cross section integrated over each line, we used the linewidths as calculated in Ref. 18 to convert to peak absorption. Our data are in good agreement with those of Refs. 10–12, although the measured α_0 of the high-frequency lines appears to be low. To indicate that they are relative values only, the last four columns are marked with asterisks. We have normalized these values with respect to the 1.097-THz transition. In order to convert the line strengths of Ref. 16 into absorption coefficients, one must take the frequency dependence, linewidth, Boltzmann factors, and spin statistical weights into account.[19] The absorption strengths of Ref. 13 are the only ones that show strong disagreement with our measurements.

As the technique described directly probes the electric field, we also obtain the measured phase shift plotted in Fig. 3(c). The Kramers–Kronig relations couple this phase shift to the absorption, and there is indeed excellent agreement between the two; as expected for a Lorentzian line, the magnitude of the jump in phase experienced at each resonance equals the peak absorption.

Two competing far-infrared spectroscopic techniques are microwave spectroscopy, based on harmonic generation and mixing, and Fourier-transform spectroscopy. With microwave techniques the frequencies of the rotational transitions of water molecules have been determined with extreme accuracy.[16] However, it is difficult to determine the line strengths, and consequently they are described by the adjectives weak and strong. Common practice is to calculate the absorption strength from a model that uses input parameters deduced from the frequency data.[10–16] In comparing time-domain spectroscopy with Fourier-transform spectroscopy, it should be clear that the frequency resolutions of these techniques are similar, as they are both based on a scanning delay line. Although for now Fourier-transform spectroscopy is superior above 1.5 THz, the limited power of the radiation sources and the problems with the thermal background favor time-domain spectroscopy below 1.0 THz.

We acknowledge informative discussions with Søren Keiding concerning the calculations of line strengths, and we thank Hoi Chan for the excellent masks and wafer fabrication. This research was partially supported by the U.S. Office of Naval Research.

References

1. A. P. DeFonzo, M. Jarwala, and C. R. Lutz, Appl. Phys. Lett. **50,** 1155 (1987); A. P. DeFonzo and C. R. Lutz, Appl. Phys. Lett. **51,** 212 (1987).
2. P. R. Smith, D. H. Auston, and M. C. Nuss, IEEE J. Quantum Electron. **24,** 255 (1988).
3. Ch. Fattinger and D. Grischkowsky, Appl. Phys. Lett. **53,** 1480 (1988); **54,** 490 (1989).
4. M. van Exter, Ch. Fattinger, and D. Grischkowsky, Appl. Phys. Lett. **55,** 337 (1989).
5. K. P. Cheung and D. H. Auston, Infrared Phys. **26,** 23 (1986).
6. D. Grischkowsky, C.-C. Chi, I. N. Duling III, W. J. Gallagher, M. B. Ketchen, and R. Sprik, in *Laser Spectroscopy VIII*, W. Persson and S. Svanberg, eds. (Springer-Verlag, New York, 1987).
7. D. Grischkowsky, in *Proceedings of the Fourth International Conference on Infrared Physics*, R. Kesselring and F. K. Kneubuhl, eds. (ETH, Zurich, 1988).
8. Y. Pastol, G. Arjavalingam, J.-M. Halbout, and G. V. Kopcsay, Appl. Phys. Lett. **54,** 307 (1989).
9. C. Johnson, F. J. Low, and A. W. Davidson, Opt. Eng. **19,** 255 (1980).
10. J. M. Flaud, C. Camy-Peyret, and R. A. Toth, *Water Vapour Line Parameters from Microwave to Medium Infrared* (Pergamon, Oxford, 1981).
11. D. E. Burch, J. Opt. Soc. Am. **58,** 1383 (1968).
12. H. J. Liebe, Radio Sci. **20,** 1069 (1985).
13. R. T. Hall, D. Vrabec, and J. M. Dowling, Appl. Opt. **5,** 1147 (1966).
14. D. E. Gray, ed., *American Institute of Physics Handbook* (McGraw-Hill, New York, 1972).
15. J. Kauppinen, T. Karkkainen, and E. Kyro, J. Mol. Spectrosc. **71,** 15 (1978).
16. F. C. De Lucia and P. Helminger, Int. J. Infrared Millim. Waves **4,** 505 (1983).
17. P. R. Griffiths, *Chemical Infrared Fourier Transform Spectroscopy* (Wiley, New York, 1975).
18. W. S. Benedict and L. D. Kaplan, J. Chem. Phys. **30,** 388 (1959).
19. C. H. Townes and A. L. Schawlow, *Microwave Spectroscopy* (McGraw-Hill, New York, 1955), see Eqs. (4-22) and (4-28).